

Early formation of the Moon 4.51 billion years ago

Melanie Barboni,^{1*} Patrick Boehnke,^{1,2} Brenhin Keller,^{3,4} Issaku E. Kohl,¹ Blair Schoene,³ Edward D. Young,¹ Kevin D. McKeegan¹

Establishing the age of the Moon is critical to understanding solar system evolution and the formation of rocky planets, including Earth. However, despite its importance, the age of the Moon has never been accurately determined. We present uranium-lead dating of Apollo 14 zircon fragments that yield highly precise, concordant ages, demonstrating that they are robust against postcocrystallization isotopic disturbances. Hafnium isotopic analyses of the same fragments show extremely low initial $^{176}\text{Hf}/^{177}\text{Hf}$ ratios corrected for cosmic ray exposure that are near the solar system initial value. Our data indicate differentiation of the lunar crust by 4.51 billion years, indicating the formation of the Moon within the first ~60 million years after the birth of the solar system.

INTRODUCTION

The surface of the Moon provides the most accessible record of planetary formation processes and the early evolution of our solar system. Geochemical analyses of Apollo samples and lunar meteorites have contributed to the present paradigm of lunar formation through a giant impact (GI) on/with the proto-Earth (1, 2), followed by rapid accretion of the orbiting debris and nearly complete melting of the proto-Moon. Chemical differentiation and crystallization of this hypothesized global lunar magma ocean (LMO) produced dense mafic cumulates that sank to the base of the LMO and a buoyant plagioclase-rich crust that formed the lunar highlands (3). Although there is consensus for this general model of lunar formation and early evolution, the timing of the GI and subsequent events remains controversial, with some planetary scientists favoring the formation within ~100 million years (My) after the formation of the solar system [4.45 billion years ago (Ga) to 4.47 Ga] (4–6) and others arguing for a relatively late GI (4.35 Ga to 4.42 Ga), approximately 150 My to 200 My after the beginning of the solar system (7–10). The “young” ages for lunar formation are difficult to reconcile with the zircon records from the Hadean era of Earth’s history (11) and from the Moon (12), which show ages as old as 4.38 Ga and 4.4 Ga, respectively. In addition, the vast majority of dynamical models are inconsistent with Moon-forming impact occurring 100 My after the birth of the solar system (13, 14). Therefore, knowledge of the age of the Moon is important not only for developing a detailed understanding of LMO duration and crystallization processes (15) but also for constraining competing models of solar system evolution during the later stages of planetary accretion.

Attempts to determine an age for the formation of the Moon can be divided into two main approaches: dating the GI event through its possible collateral effects on other solar system bodies or dating products of the solidification of the LMO itself. Various recent proposals to constrain the timing of events in relation to the GI include modeling of the addition of highly siderophile elements to Earth during the last stages of accretion (6), the timing of loss of volatile Pb relative to refractory U in the bulk silicate Earth following the GI (7), and dating of the thermal effects possibly due to the impact of numerous kilometer-sized, high-velocity fragments of GI ejecta on main-belt asteroids, as monitored by Pb loss in meteoritic apatite grains (4) or by $^{40}\text{Ar}/^{39}\text{Ar}$ age

spectra (5). An insurmountable problem with these indirect approaches is that there is no way to ascertain that the measured effects (for example, Pb isotope compositions or $^{40}\text{Ar}/^{39}\text{Ar}$ ages) are associated with the GI event. A more direct constraint on the age of the Moon can be obtained by dating the chemical differentiation events accompanying the crystallization of the LMO. This approach has been used in deriving Pb isotope model ages for the source regions of lunar basalts (10) and measuring Sm-Nd and Rb-Sr isochron ages of individual lunar rocks (7, 8). However, Pb model ages are uncertain because of poorly constrained U/Pb fractionation (high μ) on the Moon (10, 16). Similarly, isochron ages can only date the LMO solidification if all the minerals crystallized synchronously and have subsequently remained undisturbed, a remote possibility for whole-rock data, given that the analyzed Apollo lunar rocks are impact-induced breccias.

To avoid these difficulties, we use combined U-Pb and Lu-Hf isotope systematics in individual zircons crystallized from the LMO to construct a two-stage model age for the globally synchronous primary differentiation of the Moon. This has the advantage of defining the age of the Moon without complications of lunar accretion following the GI. The investigated zircon fragments are ancient, robust against later isotopic disturbance (for example, impacts and brecciation), and amenable to high-precision absolute chronology. Hafnium isotopic analysis of the same volumes of zircon dated by high-precision U-Pb geochronology document exceedingly little ingrowth of radiogenic ^{176}Hf due to the decay of ^{176}Lu in the magma from which the zircons were formed. A model differentiation age can be derived, with the assumption that initial Lu/Hf and Hf isotopic compositions in the source are known. Traditionally, a uniform chondritic composition [chondritic uniform reservoir (CHUR)] of refractory trace elements has been assumed for the Earth-Moon system, but this was called into question by the finding of ^{142}Nd discrepancies between Earth and chondrites (17), suggesting that Earth (and, by extension, the Moon) might have formed with a nonchondritic Sm-Nd. However, Burkhardt *et al.* (18) showed that this anomaly is actually the result of a small nucleosynthetic effect in Nd isotopic composition, which removes the only evidence for the Earth-Moon system deviating significantly from chondritic abundances of refractory trace elements. In addition, any nucleosynthetic effects (for example, in Hf isotopes) are thought to be small enough that they could not significantly affect Lu/Hf model ages (19). Finally, lunar zircons are thought to form in the KREEP (potassium, rare-Earth elements, and phosphorus enriched reservoir) reservoir, which formed only at the end of LMO crystallization (20). Therefore, coupled U-Pb and Hf isotopic data on lunar zircons can be used to determine the age of bulk solidification of the Moon.

2017 © The Authors,
some rights reserved;
exclusive licensee
American Association
for the Advancement
of Science. Distributed
under a Creative
Commons Attribution
NonCommercial
License 4.0 (CC BY-NC).

¹Department of Earth, Planetary, and Space Sciences, University of California, Los Angeles, Los Angeles, CA 90095, USA. ²Department of the Geophysical Sciences, The University of Chicago, Chicago, IL 60637, USA. ³Department of Geosciences, Princeton University, Princeton, NJ 08544, USA. ⁴Berkeley Geochronology Center, Berkeley, CA 94709, USA.
*Corresponding author. Email: mbarboni@epss.ucla.edu

RESULTS

For this study, we selected the remaining fragments from eight Apollo 14 zircon grains that had been previously analyzed by Taylor *et al.* (20). The zircons were separated from saw cuttings of polymict breccias 14304 and 14321 as well as from 14163, a soil sample collected from the upper few centimeters of the lunar regolith (see the Supplementary Materials for further sample descriptions). The Taylor *et al.* study (20) reported U-Pb crystallization ages obtained by secondary ion mass spectrometry (SIMS) followed by laser ablation multiple collector inductively coupled plasma MS (LA-MC-ICPMS) to determine Hf isotopic compositions and ^{176}Lu - ^{176}Hf systematics. It suggested an early formation of the Moon (before 4.5 Gy, within the first 68 My of the solar system); however, the uncertainties were permissive of an LMO crystallization age up to ~120 My after solar system origin (13). Hafnium isotope data obtained from soil sample 14163 were not included in the published study because shifts in the nonradiogenic isotope ratios suggested problems likely attributable to cosmic ray exposure effects on the lunar surface, as the soil sample was known to comprise a complex mixture of materials, with some having very long exposure ages that range over 2 Gy (21, 22). In contrast, measured exposure ages for the zircons obtained from breccia samples 14304 and 14321 are relatively short (<30 My; Supplementary Materials). Two recent studies (23, 24) have quantified the effects of neutron capture on the Hf isotope ratios, demonstrating that initial $^{176}\text{Hf}/^{177}\text{Hf}$ ratios can shift by several $\epsilon^{176}\text{Hf}(t)$ units for samples with significant exposure to cosmic radiation [note that ϵ unit = $^{176}\text{Hf}/^{177}\text{Hf}$ deviation from chondritic composition (CHUR) in parts of 10^4 for a given, identical time (t)]. An additional potential issue with the previous lunar zircon data is that the precision of the SIMS U-Pb ages was insufficient to assess concordance and thus rule out the possibility of ancient Pb loss that could bias crystallization ages to younger values. Also, SIMS U-Pb ages were determined at the very surface of the zircon (~1- μm -deep, 40- μm -diameter pit), whereas LA-MC-ICPMS used a ~200 times larger analyt-

ical volume, therefore leaving open the possibility of inaccuracies in calculating $\epsilon^{176}\text{Hf}(t)$ by not measuring Lu-Hf and U-Pb isotopes in the same volume of zircon (25). Finally, the initial value and the evolutionary trajectory of $^{176}\text{Hf}/^{177}\text{Hf}$ of the solar system (CHUR) has been recently revised by direct measurement of zircon grains from the eucrite Agoult (26) that crystallized within the first ~12 My of the solar system. This work has significantly improved the precision and accuracy with which CHUR is known and therefore allows the determination of Lu/Hf model ages with high confidence.

We used isotope dilution thermal ionization mass spectrometry (ID-TIMS) on chemically abraded zircons to obtain U-Pb dates (table S1A). Crystallization ages for our analyzed zircons extend over 365 My, from 4335 Ma to 3969 Ma, similar to the range of ages previously reported for Apollo 14 zircons by SIMS (20, 27). However, the improved precision on $^{206}\text{Pb}/^{238}\text{U}$ and $^{207}\text{Pb}/^{235}\text{U}$ dates afforded by ID-TIMS and the ability to remove zircon domains affected by Pb loss (by two leaching steps of 6 hours each at 185°C; see the Supplementary Materials) permit the use of only demonstrably closed-system zircon domains for our Hf model ages (Fig. 1). This approach is validated in that the first leaching steps yielded discordant U-Pb dates (table S1B), whereas most of the second leachates and residues are within $\pm 0.5\%$ of concordia (table S1A). One of the zircon residues (14163 z86) that displayed a small degree (2.5%) of Pb loss has a $^{207}\text{Pb}/^{206}\text{Pb}$ date that is within 13 My of its concordant second leachate, supporting the veracity of the residue age. Two other analyses that fall slightly off the concordia curve but are still used for Hf model ages are the youngest in the population (14304 z20; discordant by 1.2%) and a second leachate of 14304 z52 (0.81% discordant). From these data, we conclude that the Apollo 14 zircons chosen for Hf analysis and presented in Fig. 1 and table S1A have not experienced significant amounts of Pb loss and that the $^{207}\text{Pb}/^{206}\text{Pb}$ ages accurately reflect the timing of zircon crystallization.

We measured Hf isotopes by solution MC-ICPMS in the same volume of zircon as that used for the TIMS U-Pb dating by analyzing

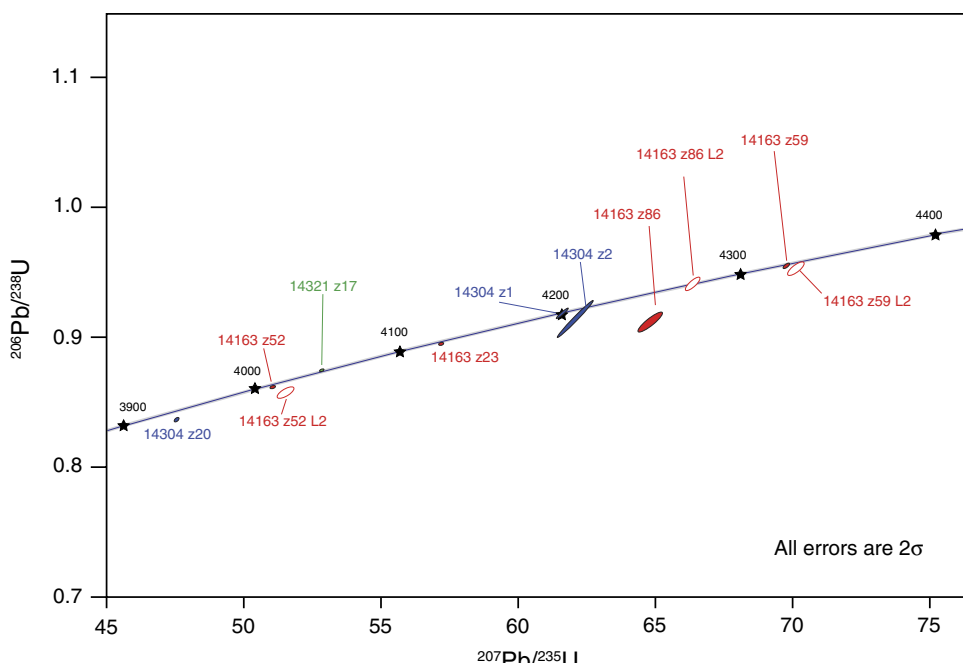


Fig. 1. Concordia diagram of the Apollo 14 zircons used to determine Hf model ages. U-Pb ID-TIMS analyses of zircon leachate (empty ellipses) and analyses of the remaining zircon residues after step leaching (filled ellipses). Ellipses are color-coded for samples.

the wash retrieved from the U-Pb chemistry (see the Supplementary Materials for analytical details). This approach allows us to unambiguously link Hf isotope compositions to the U-Pb ages (28). The Lu/Hf of each zircon was measured by ICPMS on an aliquot of the same solution to correct for in situ radiogenic growth of ^{176}Hf since zircon crystallization. The effects of possible neutron capture on the Apollo 14 zircon Hf isotopic ratios were assessed by examining the deviation of their $^{178}\text{Hf}/^{177}\text{Hf}$ ratios from normal (terrestrial and chondritic) values (24, 29). Most of our zircons [as well as the zircons analyzed by Taylor *et al.* (20)] have been affected to some degree by cosmic ray exposure with offsets up to $2.14 \epsilon^{178}\text{Hf}$ from the terrestrial value (Fig. 2). We corrected for these effects using the data and procedure of Sprung *et al.* (23), resulting in shifts between 0 and 5.6 in $\epsilon^{176}\text{Hf}(t)$ (Supplementary

Materials). The corrected initial $\epsilon^{176}\text{Hf}(t)$ values, shown as a function of crystallization age in Fig. 3, are the lowest measured in lunar materials, with the least radiogenic samples in the Apollo 14 population having initial $^{176}\text{Hf}/^{177}\text{Hf}$ ratios within 1 to 2 ϵ units (0.01 to 0.02%) of the solar system initial value (Supplementary Materials) (16). These data indicate the formation of the zircons in a highly enriched magma, termed urKREEP (30), which agrees with the previous conclusions of Taylor *et al.* (20). However, the precision of the data presented here and the corrections for cosmic ray exposure (23) that permit accurate determination of initial $\epsilon^{176}\text{Hf}(t)$ values on individual zircons with concordant U/Pb ages place tight constraints on the timing of Lu/Hf fractionation during LMO crystallization.

A model age for the separation of the LMO from the CHUR primordial reservoir is determined by calculating when the LMO zircons and the primordial Earth-Moon reservoir had the same $^{176}\text{Hf}/^{177}\text{Hf}$ ratio, which requires an estimate of the $^{176}\text{Lu}/^{177}\text{Hf}$ of the magma from which the zircon crystallized (Supplementary Materials). We chose to calculate the model ages using $^{176}\text{Lu}/^{177}\text{Hf}_{\text{source}} = 0$, which corresponds to the maximum elemental fractionation possible for the reservoir that the zircons crystallized from. Although this represents extreme Lu/Hf fractionation, it is reasonably consistent with expectations for fractional crystallization of an LMO and production of zircon in the last residual melt (urKREEP). A pMELTS simulation (31) with the alphaMELTS interface (32) of $^{176}\text{Lu}/^{177}\text{Hf}$ during KREEP crystallization shows that it quickly evolves to <0.01 at less than 50% melt remaining (Supplementary Materials). Any choice of a higher Lu/Hf ratio for the source necessarily yields older model separation ages; our results therefore provide minimum ages for differentiation of the LMO from CHUR and a minimum age for the formation of the Moon. Our model age results are presented in Fig. 4, together with those from Taylor *et al.* (20) corrected for neutron capture effects. Because some of the Apollo 14 zircons with initial $\epsilon^{176}\text{Hf}(t)$ values closer to chondritic could be derived from KREEP-rich magmas that had undergone partial assimilation of crustal rocks, we take the oldest model ages as the minimum age for LMO solidification. To determine this minimum age, we averaged the four oldest zircon Lu/Hf model ages, resulting in 4.51 ± 0.01 Gy (1σ).

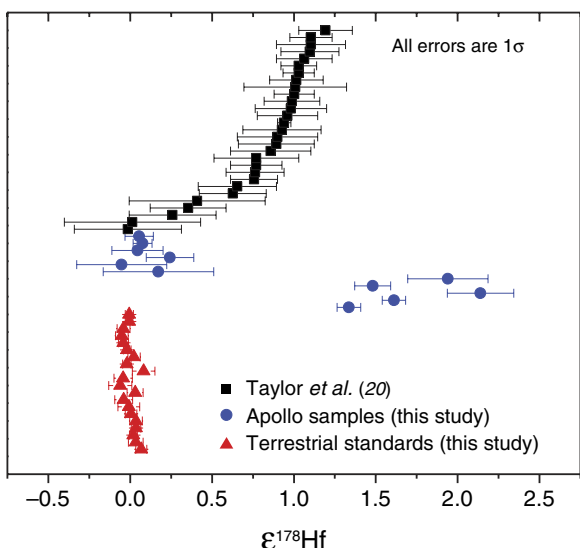


Fig. 2. Magnitude of the neutron capture effect on Apollo zircons as shown by the shift in $^{178}\text{Hf}/^{177}\text{Hf}$. The shift is expressed as a deviation in $\epsilon^{178}\text{Hf}$ s from the terrestrial value (56). Samples with a large offset in $\epsilon^{178}\text{Hf}$ all come from soil 14163 that experienced longer cosmic ray exposure on the near surface of the Moon.

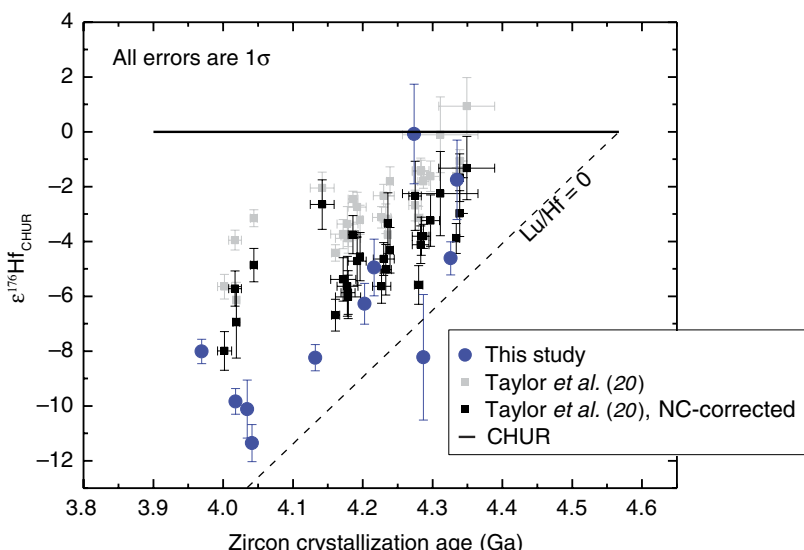


Fig. 3. Plot of $\epsilon^{176}\text{Hf}_{\text{CHUR}}$ versus $^{207}\text{Pb}/^{206}\text{Pb}$ zircon age (Gy). $\epsilon^{176}\text{Hf}_{\text{CHUR}}$ is evaluated by the difference between initial $\epsilon^{176}\text{Hf}(t)$ and the Hf isotopic composition of CHUR at time t (26). Taylor *et al.* (20) reported the data before and after neutron capture (NC) correction.

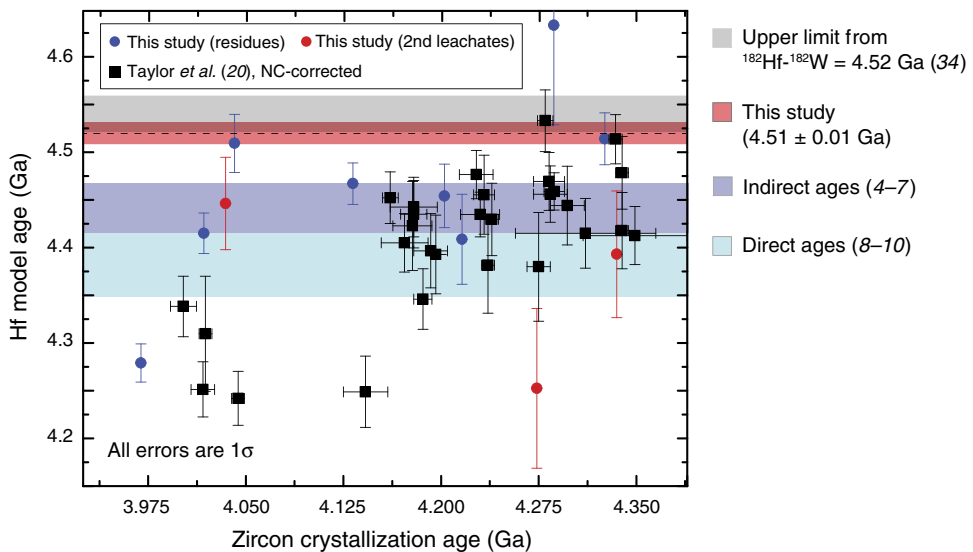


Fig. 4. Hf model age (Gy) calculated for a $\text{Lu/Hf}_{\text{source}} = 0$ as a function of $^{207}\text{Pb}/^{206}\text{Pb}$ zircon crystallization age (Gy). Ranges of previously proposed ages for the Moon's formation are also shown.

DISCUSSION

Our model age is ~120 My to 150 My older than estimates based on Sm-Nd and Pb-Pb isochrons measured on ferroan anorthosites that are thought to represent early floatation cumulates of LMO crystallization (8) and dating of Mg suite lunar crustal rocks (9). We reiterate that our model age for differentiation of the LMO is actually a minimum estimate for the age of the Moon because we took the lowest possible value for Lu/Hf in the source reservoir ($\text{Lu/Hf}_{\text{source}} = 0$). Furthermore, previous uncertainties regarding the chondritic nature of the Moon and the evolution of Hf isotopes in chondrites (CHUR) have recently been addressed (26). Therefore, the zircon Hf model ages are accurately related to an absolute time scale. Our data unambiguously show that the Moon was differentiated and mostly solidified by 4.51 Gy, so the young ages obtained on lunar highland samples cannot be directly dating the age of the Moon. If these Sm-Nd ages are not compromised by later disturbances, including brecciation and shocks, they may reflect the time of slow cooling through the low closure temperature of the Sm-Nd system (33). However, if these limitations do not apply and the Moon cooled quickly, then a reexamination of the origin of ferroan anorthosites in the context of the LMO hypothesis is required, as suggested by Borg *et al.* (8). Our results are consistent with constraints given by the short-lived $^{182}\text{Hf}-^{182}\text{W}$ system that indicate that the formation of the Moon must have occurred later than ~50 My after the beginning of the solar system (34). Because the Hf isotopic composition of the lunar zircons requires solidification of the LMO by ~4.51 Gy, we conclude that the GI and formation of the Earth-Moon system must have occurred within the first ~60 My of the formation of the solar system, with an uncertainty on the order of 10 My (1σ).

MATERIALS AND METHODS

Sample description

We analyzed the fragments of eight zircons that were previously separated at the University of California, Los Angeles (UCLA) from Apollo 14 samples by Taylor *et al.* (20). Four zircons were derived from 14163, a soil sample representing the upper few centimeters of the lunar regolith. Cosmic ray exposure ages reported for 14163 soil particles (22)

and partnered sample 14161 (21) ranged from 100 My to 2.5 Gy, indicative of a complex mixture of materials that have been cycled through the regolith, perhaps repeatedly, over a long period. Analyses of zircons from this sample were not included in the published study of Taylor *et al.* (20) because it was recognized that the long exposure age may have compromised Hf isotopic compositions through neutron capture reactions and, at the time, there was no method available to quantitatively correct for these effects. In the intervening time, Sprung *et al.* (23, 24) determined neutron capture effects on Hf isotope ratios so that we can now use correlated isotope ratios to accurately correct measured $^{176}\text{Hf}/^{177}\text{Hf}$ in each zircon (see the “Lu-Hf parameters and model age calculation” section). Three zircons analyzed here and reported by Taylor *et al.* (20) were found among saw cuttings from the interior of rock 14304, a ~2.5-kg polymict breccia that was almost completely buried in the regolith at the time of collection. No cosmic ray exposure ages have been determined on 14304; however, exposure ages were measured on 14305, a nearby, similarly sized rock. The exposure ages for 14305 range from 11 My (by the ^{129}Xe method) (35) to 28 My (by the ^{81}Kr method) (36). The final zircon reported here was obtained from saw cuttings of 14321, a complex polymict breccia that, at 9 kg, was the largest rock returned by Apollo 14 (37). The sample was partially buried in the ejecta blanket of Cone Crater, a relatively young [26 My (38)] crater that excavated material from the Fra Mauro formation that is thought to sample material from the Imbrium impact basin. Cosmic ray exposure ages of 14321 averaged 24 My, consistent with the age of the Cone Crater. SIMS U/Pb ages previously obtained from zircons from 14321 range from 4.01 Gy to 4.33 Gy (39, 40).

U-Pb geochronology

Individual zircon fragments were removed from epoxy mounts and thermally annealed by transferring the fragments into quartz crucibles and heated to 900°C for 48 hours. The fragments were then rinsed with acetone in 3-ml Savillex PFA (fluoropolymer) beakers, fluxed in 6 M HCl for 1 hour at 100°C, and rinsed again using MQ H₂O. The zircon fragments were then loaded into 200-μl Savillex microcapsules with 100 μl of 29 M HF + 15 μl of 3 M HNO₃ for the first step of chemical abrasion (41) in high-pressure Parr bombs for 6 hours at 185°C.

Grains were rinsed 10 times after the first-step leaching with 6 M HCl, MQ H₂O, and 29 M HF before being leached again with 100 µl of 29 M HF + 15 µl of 3 M HNO₃ for a second 6-hour step of chemical abrasion at 185°C. The same rinsing procedure done for the first-step leaching was also applied after the second-step leaching. Both leachates from the first and second steps (subsequently referred to as L1 and L2) were saved (21). L1 samples were spiked with the EARTHTIME ²⁰⁵Pb-²³³U-²³⁵U tracer (42, 43), and zircon fragment residues and L2 samples were spiked with the EARTHTIME ²⁰²Pb-²⁰⁵Pb-²³³U-²³⁵U tracer (42, 43). The remaining zircon fragments (subsequently referred to as “residues”) were then dissolved to completion in 100 µl of 29 M HF + 15 µl of 3 N HNO₃ in Parr bombs for 48 hours at 210°C. Leachates L1 and L2 were individually dried down and converted to chlorides by overnight redissolution using 100 µl of 6 N HCl in Parr bombs at 185°C. All samples (L1, L2, and residues) were subsequently dried down and brought up in 50 µl of 3 M HCl. The U-Pb and trace element aliquots (including Lu-Hf) were separated by anion exchange column chromatography using a modified single 50-µl column and AG 1-X8 resin [200- to 400-mesh chloride from Eichrom (44)]. The trace element aliquot (including Hafnium) was saved for multi- and single-collector ICPMS analysis. The U-Pb aliquots were collected in single beakers, dried down with a drop of 0.02 M H₃PO₄, and analyzed on a single outgassed zone-refined Re filament in a Si gel emitter (45).

Isotopic measurements were performed on an Isotopx Phoenix62 TIMS at Princeton University. Pb was measured in dynamic mode on an axial ion-counting Daly photomultiplier. Dead time for the Daly was determined to be 40.5 ns during the period of analysis by repeated measurements of the NBS-981 and NBS-982 standard at up to 2.5 million counts per second. A correction for mass-dependent Pb fractionation was applied as follows. For analyses performed using the EARTHTIME ²⁰²Pb-²⁰⁵Pb-²³³U-²³⁵U “double-Pb” tracer (L2 and residues), a cycle-by-cycle fractionation correction was calculated from the deviation of measured ²⁰²Pb/²⁰⁵Pb from the known tracer ²⁰²Pb/²⁰⁵Pb [0.99924 ± 0.00027 (1σ)]. For analyses performed using the EARTHTIME ²⁰⁵Pb-²³³U-²³⁵U “single-Pb” tracer (L1), a Pb fractionation of 0.16 ± 0.02% per atomic mass unit (1σ) was used, as determined by repeat measurement of NBS-981 and NBS-982 and verified by those spiked with the double-Pb tracer. Baseline measurements were made at each half-mass, and the average intensity bounding each measured peak was subtracted. Isobaric interferences of BaPO₄ and Tl on sample Pb isotopes were monitored and corrected for by measuring masses 203 and 201. No corrections were applied for the L1 leachates analyzed with the EARTHTIME ²⁰⁵Pb-²³³U-²³⁵U, with the decay of mass 203 over the duration used as an indicator of declining isobaric interferences under all Pb masses. Corrections were applied to analyses using the EARTHTIME ²⁰²Pb-²⁰⁵Pb-²³³U-²³⁵U in the data reduction software Tripoli (46), using version 1 isotopic composition models for both species (www.earth-time.org). Data culling was done in this same program using the decreasing 203/205 and the increasing 206/204 ratios over the course of an analysis.

Depending on the sample intensities, U was measured in either static mode on Faraday cups on 10¹²-ohm resistors or dynamic mode on the Daly photomultiplier (dead time determined at 32.75 ns by repeated measurements of CRM U500). Uranium species were measured as UO₂⁺, ²³³UO₂, and ²³⁵UO₂ and were corrected for an oxygen isotopic composition of 0.002055 [see discussion by McLean *et al.* (43)]. Because ¹⁸O/¹⁶O typically grows at the beginning of an analysis before stabilizing, early blocks of data were deleted. Baselines for static analyses were measured at ±0.5 mass units for 30 s every 30 ratios. Correction for mass fractionation of U was done using the EARTHTIME ²⁰⁵Pb-²³³U-²³⁵U

and EARTHTIME ²⁰²Pb-²⁰⁵Pb-²³³U-²³⁵U tracer solutions, assuming a sample ²³⁸U/²³⁵U ratio of 137.818 ± 0.021 (47). Variable ²³⁸U/²³⁵U was measured on Earth and meteorites, and changing the sample ²³⁸U/²³⁵U within those ranges can change the ²⁰⁷Pb/²⁰⁶Pb ages by several million years. However, this is not a significant source of uncertainty in the Hf model ages and therefore do not affect our age-of-moon analysis. We also note that uranium blanks could have a significant effect on the concordance of very low U grains. However, a sensitivity test performed by varying the U blanks from 0.009 to 0.09 pg shows that the U blank composition is not important for the concordant and radiogenic grains that are included in the age-of-moon analysis (table S1A).

All data reduction, error propagation, and U-Pb data plotting were done using the U-Pb_Redux software package (48). All reported uncertainties were 2σ and included only internal sources of uncertainty (counting statistics, uncertainties in correcting for mass discrimination, and the uncertainty in common Pb composition). Forty procedural blanks spiked with the same tracers and run within a period of 3 years (21 of which in the course of this study) showed an amount of common Pb (Pbc = 0.2 to 13.9 pg; average, 3.6 pg) that agreed well with that found in zircon analyses; therefore, all common Pb was assumed to be derived from procedural blanks. The composition of the 40 spiked blanks is as follows: ²⁰⁶Pb/²⁰⁴Pb = 18.44 ± 0.18, ²⁰⁷Pb/²⁰⁴Pb = 15.53 ± 0.18, and ²⁰⁸Pb/²⁰⁴Pb = 37.38 ± 0.53 (2σ SD); these uncertainties were propagated into each U-Pb analysis. Data are presented in table S1 (A and B). U-Pb results show that L1 and some of L2 analyses had low radiogenic-to-common Pb ratios and were discordant (table S1B), whereas most of the residues and L2 have high radiogenic-to-common Pb ratios and are concordant (table S1A). This illustrates that the chemical abrasion technique efficiently removed portion of grains that were affected by Pb loss. Hf measurements were performed only on the most concordant grains (tables S1A and S3), which are plotted on Fig. 1 in a traditional concordia plot.

Hf isotope analytical procedure

Hf isotopic compositions were determined for the eight zircon residues and three of the L2 (14163_z86_L2, 14163_z59_L2, and 14163_z52_L2) aliquots that were separated during the TIMS U-Pb chemistry procedure (showing concordance or near concordance; see above and Fig. 1). Analyses were made by solution of MC-ICPMS on the ThermoFinnigan Neptune at UCLA using a Cetac “Aridus II” desolvating nebulizer. Analyses were done without matrix purification following the analytical protocol of D’Abzac *et al.* (49). Analytical parameters were summarized in table S2, and data were presented in table S3 (A and B). Ions were collected from masses 171, 173, 174, 175, 176, 177, 178, 179, and 181 simultaneously in nine Faraday cups (10¹¹-ohm resistors) to perform peak stripping of the interfering masses (¹⁷⁶Yb⁺ and ¹⁷⁶Lu⁺ with ¹⁷⁶Hf⁺). Blanks were measured before every lunar zircon analysis after washing the line for 6 min and were subtracted from the sample counts. The amount of ¹⁷⁶Yb⁺ subtracted from the total signal at mass 176 was calculated cycle by cycle from the ¹⁷¹Yb⁺ intensity corrected for mass fractionation and assuming a normal ¹⁷⁶Yb/¹⁷¹Yb ratio [0.901821 (50)]. Similarly, the amount of ¹⁷⁶Lu⁺ to be stripped was calculated from the measured ¹⁷⁵Lu⁺, normalized to ¹⁷⁶Lu/¹⁷⁵Lu [0.026549 (50)]. Instrumental mass bias correction for Yb and Hf (β_{Yb} and β_{Hf}) was internally calculated cycle by cycle from the measured ¹⁷³Yb/¹⁷¹Yb and ¹⁷⁹Hf/¹⁷⁷Hf ratios using the exponential fractionation law. β_{Lu} was determined by multiple analyses of the NIST 3130a Lu standard solution, which we doped with Zr to match our solutions; variations in β_{Lu} accounted for changes of <0.1 ε in ¹⁷⁶Hf/¹⁷⁷Hf and were therefore negligible. Data are presented in table S3A.

To test the accuracy of the peak stripping procedure, we performed multiple analyses of three dissolved natural zircon standards [AS3, 91500, and Mudtank (51)], four dissolved synthetic zircons variably doped with REE [MUNZirc 0, 1, 3, and 4 (52)], and the SPEX-1 Hf solution from CertiPrep. These samples covered a large range in Lu/Hf and Yb/Hf (0 to 0.098 and 0 to 0.645, respectively), up to values matching the ratios of the lunar zircons. Five standards were run at the start of each analysis session, several more were interspersed between lunar zircon measurements, and five were again measured at the end of the session. Standard analyses are presented in table S3B. Our measured mean value of $^{176}\text{Hf}/^{177}\text{Hf}$ for all the standards was offset by an average of $-0.54 \pm 0.18 \epsilon$ from the published values. Because this offset was constant for all the standard zircons, we corrected all measured $^{176}\text{Hf}/^{177}\text{Hf}$ for this factor after peak stripping. That there was no remaining systematic error due to the peak stripping can be seen in fig. S1, which shows that all standard zircons plot within the error of their respective $^{176}\text{Hf}/^{177}\text{Hf}$ values (expected values from literature) even with the magnitude of the $^{176}\text{Yb}^+$ interference varying by four orders of magnitude. Because our standards encompassed the full range of Yb/Hf concentrations seen in the Apollo 14 zircons, we were confident of the accuracy of the $^{176}\text{Hf}/^{177}\text{Hf}$ determinations within the stated precision. The reproducibility of $\sim 0.2 \epsilon$ measured for the standards was propagated in our uncertainties on the Apollo samples (see section below). Additional tests were performed to check for errors arising from low-intensity signals by diluting concentrations of standards to match the lowest intensities we observed in the lunar samples (see table S3B). No systematic effects were found outside of quoted uncertainties. We finally note that D'Abzac *et al.* (49) reported significant impact of Yb oxides on the peak-stripped $^{176}\text{Hf}/^{177}\text{Hf}$ ratios due to the changing mass fractionation exponent, β_{Yb} . We did not observe such effects in our analytical session and believed that this difference is attributable to the different behavior of the cones (53), as D'Abzac *et al.* (49) used the "jet" skimmer cone, whereas we used the "x" cones.

Model age calculation

Lu-Hf parameters and model age calculation.

We used the Lu-Hf parameters for CHUR, as recently determined by Iizuka *et al.* (26), with a best solar system initial value of $^{176}\text{Hf}/^{177}\text{Hf} = 0.279781 \pm 0.000018$, and took the decay constant for ^{176}Lu determined by Scherer *et al.* (29) ($\lambda_{^{176}\text{Lu}} = 1.867 \times 10^{-11} \text{ year}^{-1}$). Each zircon was corrected for the ingrowth of ^{176}Hf over the age of the zircon due to the small amount of ^{176}Lu incorporated in the zircon by using the zircon U-Pb age determined by TIMS and the measured zircon Lu/Hf. The Lu/Hf ratios were determined for every zircon and leachate by analyses of the remaining solution after Hf isotope measurements. These analyses were conducted at Princeton University on a ThermoFinnigan Element 2 ICPMS and with a 2% standard reproducibility (six analyses of MUNZirc 3 standard solution), which was propagated into the overall uncertainties (see section below). Individual model ages for each zircon can be calculated by passing a line through the measured data point using a slope based on an estimated $^{176}\text{Lu}/^{177}\text{Hf}$ of the source and finding the intersection with the chondritic evolution line (CHUR). As stated in the text, we chose to calculate the model ages using $^{176}\text{Lu}/^{177}\text{Hf}_{\text{source}} = 0$ to model the most extreme fractionation possible for the reservoir and get the absolute minimum ages for its closure (diagram of $^{176}\text{Hf}/^{177}\text{Hf}$ versus age showing the two-step model age calculation presented in fig. S2). Taking the higher Lu/Hf ratios yields older model ages (fig. S3). We present the minimum age for the Moon as permitted by the Lu/Hf system. One zircon residue (14163 z86) yields an $\epsilon^{176}\text{Hf}(t)$ that is

apparently lower than the solar system initial (Figs. 3 and 4), but note that its great uncertainty, due to the small size of the grain, overlaps allowed solar system values. This zircon was not included in the average model age of 4.51 Gy. Data are presented in table S3A.

pMELTS modeling.

It has been suggested that the Apollo zircons crystallized from KREEP. We performed pMELTS simulations (31) using the alphaMELTS interface (32) to model the crystallization of KREEP and the evolution of the Lu/Hf ratio to the last residual melt present in the KREEP reservoir. We assumed closed system crystallization under isobaric condition (5 kbar was chosen for our runs), regulated by the QFM-5 (iron-wustite) and QFM-4 oxygen fugacity buffer. We used a starting liquid equivalent to the KREEP whole-rock composition reported by Warren (54) and the KREEP Lu and Hf abundances reported by Neal and Kramer (55). We used the modal phases predicted by pMELTS together with partition coefficients from the earthref.org database to model the evolution of $^{176}\text{Lu}/^{177}\text{Hf}$ with decreasing melt content and observed that this ratio quickly becomes < 0.01 below 50% melt and < 0.001 in the last fraction melt (fig. S4), suggesting that the Moon can have a low $^{176}\text{Lu}/^{177}\text{Hf}_{\text{source}}$ reservoir.

Effect of neutron capture on the Hf isotopic ratios.

Neutron capture can shift initial $^{176}\text{Hf}/^{177}\text{Hf}$ ratios by several ϵ units, depending on exposure conditions (duration and energy). The most significant reactions affecting the Hf isotope ratios are $^{177}\text{Hf}(n,\gamma)^{178}\text{Hf}$ and $^{178}\text{Hf}(n,\gamma)^{179}\text{Hf}$ (23, 24). The problem that neutron capture creates for $\epsilon^{176}\text{Hf}$ determination is primarily in the mass bias correction because neutron capture can produce an elevated $^{179}\text{Hf}/^{177}\text{Hf}$ (23). We measured $^{178}\text{Hf}/^{177}\text{Hf}$ in the Apollo zircons and observed offsets up to 2.14ϵ from the terrestrial value (56). We corrected for these effects using the data and procedure of Sprung *et al.* (23), and this correction resulted in shifts between 0 and $5.6 \epsilon^{176}\text{Hf}(t)$ on the Apollo 14 zircons. We fitted the shift in $\epsilon^{176}\text{Hf}(t)$ of the lunar basalt data reported by Sprung *et al.* (23) versus the offset in $\epsilon^{178}\text{Hf}$ with a linear regression and applied it to our zircon data.

Error propagation.

Each analysis was reduced on a cycle-by-cycle basis for instrumental effects (that is, mass fractionation and peak stripping) through bootstrapping (57). That is to say, we used the following procedure for each sample: (i) We resampled the 80 cycles with replacement (duplicates are allowed); (ii) We corrected each cycle for interfering masses and mass fractionation; (iii) We averaged the final isotope ratios; (iv) We repeated steps (i) to (iii) 10,000 times and saved the average of this grand data set and its SD. Once each analysis was corrected for instrumental/analytical effects, we corrected each sample for neutron exposure, ^{176}Hf ingrowth, and the $-0.47 \epsilon^{176}\text{Hf}$ offset from our standard analyses. Each uncertainty (including uncertainties on neutron capture, Lu/Hf measurements, and standard analyses) was incorporated using bootstrap resampling; that is, we randomly sampled a measured value for each sample as well as that for any correction and repeated the procedure 10,000 times to calculate the final uncertainty. Our approach is analogous to using a Monte Carlo procedure to propagate the uncertainties.

SUPPLEMENTARY MATERIALS

Supplementary material for this article is available at <http://advances.sciencemag.org/cgi/content/full/3/1/e1602365/DC1>

fig. S1. $^{176}\text{Hf}/^{177}\text{Hf}$ ratios normalized to the expected (present-day) value for standard zircons versus the magnitude of the peak stripping due to interfering Yb, measured as $^{173}\text{Yb}^+/^{177}\text{Hf}^+$.

fig. S2. Initial $^{176}\text{Hf}/^{177}\text{Hf}$ of Apollo 14 zircons versus absolute time (My) and time after the start of the solar system [calcium- and aluminum-rich inclusions (CAIs)] in millions of years.

- fig. S3. Hf model age variations depending on the $^{176}\text{Lu}/^{177}\text{Hf}$ ratios for the source.
- fig. S4. KREEP $^{176}\text{Lu}/^{177}\text{Hf}$ evolutions through decreasing melt percent, as given by pMELTS simulations.
- table S1A. U-Pb isotopic data (zircons also measured for Hf isotope composition and used for the determination of the age of the Moon).
- table S1B. U-Pb isotopic data (zircons not measured for Hf isotope composition).
- table S2. Tuning parameters of the coupled Cetac "Aridus II" and ThermoFinnigan Neptune MC-ICPMS.
- table S3A. Hf isotopic data and model age calculations for lunar zircons.
- table S3B. Summary of Hf isotopes measured on terrestrial standards.
- References (58, 59)

REFERENCES AND NOTES

1. A. G. W. Cameron, W. R. Ward, The origin of the Moon. *Proc. Lunar Planet. Sci. Conf.* **7**, 120–122 (1976).
2. M. Ćuk, S. T. Stewart, Making the Moon from a fast-spinning Earth: A giant impact followed by resonant despinning. *Science* **338**, 1047–1052 (2012).
3. J. A. Wood, J. S. Dickey Jr., U. B. Marvin, B. N. Powell, Lunar anorthosites and a geophysical model of the Moon, *Proceedings of the Apollo 11 Lunar Science Conference*, Houston, Texas, 5 to 8 January 1970 (Pergamon Press, 1970), pp. 965–988.
4. Q.-Z. Yin, Q. Zhou, Q.-L. Li, X.-H. Li, Y. Liu, G.-Q. Tang, A. N. Krot, P. Jenniskens, Records of the Moon-forming impact and the 470 Ma disruption of the L chondrite parent body in the asteroid belt from U-Pb apatite ages of Novato (L6). *Meteorit. Planet. Sci.* **49**, 1426–1439 (2014).
5. W. F. Bottke, D. Vokrouhlický, S. Marchi, T. Swindle, E. R. D. Scott, J. R. Weirich, H. Levison, Dating the Moon-forming impact event with asteroidal meteorites. *Science* **348**, 321–323 (2015).
6. S. A. Jacobson, A. Morbidelli, S. N. Raymond, D. P. O'Brien, K. J. Walsh, D. C. Rubie, Highly siderophile elements in Earth's mantle as a clock for the Moon-forming impact. *Nature* **508**, 84–87 (2014).
7. J. N. Connelly, M. Bizzarro, Lead isotope evidence for a young formation age of the Earth–Moon system. *Earth Planet. Sci. Lett.* **452**, 36–43 (2016).
8. L. E. Borg, J. N. Connelly, M. Boyet, R. W. Carlson, Chronological evidence that the Moon is either young or did not have a global magma ocean. *Nature* **477**, 70–72 (2011).
9. R. W. Carlson, L. E. Borg, A. M. Gaffney, M. Boyet, Rb-Sr, Sm-Nd and Lu-Hf isotope systematics of the lunar Mg-suite: The age of the lunar crust and its relation to the time of Moon formation. *Philos. Trans. A Math. Phys. Eng. Sci.* **372**, 20130246 (2014).
10. J. F. Snape, A. A. Nemchin, J. J. Bellucci, M. J. Whitehouse, R. Tartese, J. J. Barnes, M. Anand, I. A. Crawford, K. H. Joy, Lunar basalt chronology, mantle differentiation and implications for determining the age of the Moon. *Earth Planet. Sci. Lett.* **451**, 149–158 (2016).
11. T. M. Harrison, The Hadean crust: Evidence from >4 Ga zircons. *Annu. Rev. Earth Planet. Sci.* **37**, 479–505 (2009).
12. A. Nemchin, N. Timms, R. Pidgeon, T. Geisler, S. Reddy, C. Meyer, Timing of crystallization of the lunar magma ocean constrained by the oldest zircon. *Nat. Geosci.* **2**, 133–136 (2009).
13. E. D. Young, I. E. Kohl, P. H. Warren, D. C. Rubie, S. A. Jacobson, A. Morbidelli, Oxygen isotopic evidence for vigorous mixing during the Moon-forming giant impact. *Science* **351**, 493–496 (2016).
14. S. A. Jacobson, K. J. Walsh, Earth and terrestrial planet formation, in *The Early Earth: Accretion and Differentiation*, J. Badro, M. Walter, Eds. (John Wiley & Sons Inc., 2015), 49 pp.
15. L. T. Elkins-Tanton, S. Burgess, Q.-Z. Yin, The lunar magma ocean: Reconciling the solidification process with lunar petrology and geochronology. *Earth Planet. Sci. Lett.* **304**, 326–336 (2011).
16. W. Compston, I. S. Williams, C. Meyer, U-Pb geochronology of zircons from lunar breccia 73217 using a sensitive high mass-resolution ion microprobe. *J. Geophys. Res. Solid Earth* **89**, B525–B534 (1984).
17. M. Boyet, R. W. Carlson, ^{142}Nd evidence for early (>4.53 Ga) global differentiation of the silicate Earth. *Science* **309**, 576–581 (2005).
18. C. Burkhardt, L. E. Borg, G. A. Brennecke, Q. R. Shollenberger, N. Dauphas, T. Kleine, A nucleosynthetic origin for the Earth's anomalous ^{142}Nd composition. *Nature* **537**, 394–398 (2016).
19. W. Akram, M. Schönbächler, P. Sprung, N. Vogel, Zirconium—Hafnium isotope evidence from meteorites for the decoupled synthesis of light and heavy neutron-rich nuclei. *Astrophys. J.* **777**, 169 (2013).
20. D. J. Taylor, K. D. McKeegan, T. M. Harrison, Lu-Hf zircon evidence for rapid lunar differentiation. *Earth Planet. Sci. Lett.* **279**, 157–164 (2009).
21. T. Kirsten, J. Deubner, P. Horn, I. Kaneoka, J. Kiko, O. A. Schaeffer, S. K. Thio, The rare gas record of Apollo 14 and 15 samples. *Proc. Lunar Sci. Conf.* **3**, 1865–1889 (1972).
22. J. Levine, P. R. Renne, R. A. Muller, Solar and cosmogenic argon in dated lunar impact spherules. *Geochim. Cosmochim. Acta* **71**, 1624–1635 (2007).
23. P. Sprung, T. Kleine, E. E. Scherer, Isotopic evidence for chondritic Lu/Hf and Sm/Nd of the Moon. *Earth Planet. Sci. Lett.* **380**, 77–87 (2013).
24. P. Sprung, E. E. Scherer, D. Upadhyay, I. Leya, K. Mezger, Non-nucleosynthetic heterogeneity in non-radiogenic stable Hf isotopes: Implications for early solar system chronology. *Earth Planet. Sci. Lett.* **295**, 1–11 (2010).
25. T. M. Harrison, J. Blachert-Toft, W. Müller, F. Albarede, P. Holden, S. J. Mojzsis, Heterogeneous Hadean hafnium: Evidence of continental crust at 4.4 to 4.5 Ga. *Science* **310**, 1947–1950 (2005).
26. T. Izuka, T. Yamaguchi, Y. Hibiya, Y. Amelin, Meteorite zircon constraints on the bulk Lu-Hf isotope composition and early differentiation of the Earth. *Proc. Natl. Acad. Sci. U.S.A.* **112**, 5331–5336 (2015).
27. A. A. Nemchin, R. T. Pidgeon, M. J. Whitehouse, J. P. Vaughan, C. Meyer, SIMS U-Pb study of zircon from Apollo 14 and 17 breccias: Implications for the evolution of lunar KREEP. *Geochim. Cosmochim. Acta* **72**, 668–689 (2008).
28. Y. Amelin, D.-C. Lee, A. N. Halliday, R. T. Pidgeon, Nature of the Earth's earliest crust from hafnium isotopes in single detrital zircons. *Nature* **399**, 252–255 (1999).
29. E. E. Scherer, C. Münker, K. Mezger, Calibration of the lutetium-hafnium clock. *Science* **293**, 683–687 (2001).
30. P. H. Warren, J. T. Wasson, The origin of KREEP. *Rev. Geophys.* **17**, 73–88 (1979).
31. M. S. Ghiorso, M. M. Hirschmann, P. W. Reiners, V. C. Kress III, The pMELTS: A revision of MELTS for improved calculation of phase relations and major element partitioning related to partial melting of the mantle to 3 GPa. *Geochim. Geophys. Geosyst.* **3**, 1–35 (2002).
32. P. M. Smith, P. D. Asimow, Adiabat_1ph: A new public front-end to the MELTS, pMELTS, and pHMELTS models. *Geochim. Geophys. Geosyst.* **6**, Q02004 (2005).
33. P. H. Warren, P. Boehnke, Precise igneous crystallization ages for ferroan anorthosites: Merely difficult, or impossible? *Proc. Lunar Planet. Sci. Conf.* **1903**, 2997 (2016).
34. M. Touboul, T. Kleine, B. Bourdon, H. Palme, R. Wieler, Late formation and prolonged differentiation of the Moon inferred from W isotopes in lunar metals. *Nature* **450**, 1206–1209 (2007).
35. The Lunar Sample Preliminary Examination Team, Preliminary examination of lunar samples from Apollo 14. *Science* **173**, 681–693 (1971).
36. O. Eugster, P. Eberhardt, J. Geiss, N. Grögler, M. Jungck, F. Meier, M. Mörgeli, F. Niederer, Cosmic ray exposure histories of Apollo 14, Apollo 15, and Apollo 16 rocks. *J. Geophys. Res.* **89**, B498–B512 (1984).
37. C. Meyer, 14321: Clast-rich, crystalline matrix breccia, *Lunar Sample Compendium* (2003); <http://www.curator.jsc.nasa.gov/lunar/compendium.cfm>.
38. C. J. Morgan, "Exposure age dating of lunar features: Lunar heavy rare gases," thesis, Washington University, Saint Louis, MO (1975).
39. C. Meyer, I. S. Williams, W. Compston, Uranium-lead ages for lunar zircons: Evidence for a prolonged period of granophyre formation from 4.32 to 3.88 GA. *Meteorit. Planet. Sci.* **31**, 370–387 (1996).
40. M. L. Grange, R. T. Pidgeon, A. A. Nemchin, N. E. Timms, C. Meyer, Interpreting U-Pb data from primary and secondary features in lunar zircon. *Geochim. Cosmochim. Acta* **101**, 112–132 (2013).
41. J. M. Mattinson, Zircon U-Pb chemical-abrasion ("CA-TIMS") method: Combined annealing and multi-step dissolution analysis for improved precision and accuracy of zircon ages. *Chem. Geol.* **220**, 47–66 (2005).
42. D. J. Condon, B. Schoene, N. M. McLean, S. A. Bowring, R. R. Parrish, Metrology and traceability of U-Pb isotope dilution geochronology (EARTHTIME Tracer Calibration Part I). *Geochim. Cosmochim. Acta* **164**, 464–480 (2015).
43. N. M. McLean, D. C. Condon, B. Schoene, S. A. Bowring, Evaluating uncertainties in the calibration of isotopic reference materials and multi-element isotopic tracers (EARTHTIME Tracer Calibration Part II). *Geochim. Cosmochim. Acta* **164**, 481–501 (2015).
44. T. E. Krogh, A low-contamination method for hydrothermal decomposition of zircon and extraction of U and Pb for isotopic age determinations. *Geochim. Cosmochim. Acta* **37**, 485–494 (1973).
45. H. Gerstenberger, G. Haase, A highly effective emitter substance for mass spectrometric Pb isotope ratio determinations. *Chem. Geol.* **136**, 309–312 (1997).
46. J. F. Bowring, N. M. McLean, S. A. Bowring, Engineering cyber infrastructure for U-Pb geochronology: Tripoli and U-Pb_Redux. *Geochim. Geophys. Geosyst.* **12**, Q0AA19 (2011).
47. J. Hiess, D. J. Condon, N. M. McLean, S. R. Noble, $^{238}\text{U}/^{235}\text{U}$ systematics in terrestrial uranium-bearing minerals. *Science* **335**, 1610–1614 (2012).
48. N. M. McLean, J. F. Bowring, S. A. Bowring, An algorithm for U-Pb isotope dilution data reduction and uncertainty propagation. *Geochim. Geophys. Geosyst.* **12**, Q0AA18 (2011).
49. F.-X. D'Abzac, J. H. F. L. Davies, J.-F. Wotzlaw, U. Schaltegger, Hf isotope analysis of small zircon and baddeleyite grains by conventional multi collector-inductively coupled plasma-mass spectrometry. *Chem. Geol.* **433**, 12–23 (2016).
50. N.-C. Chu, R. N. Taylor, V. Chavagnac, R. W. Nesbitt, R. M. Boella, J. A. Milton, C. R. German, G. Bayon, K. Burton, Hf isotope ratio analysis using multi-collector inductively coupled plasma mass spectrometry: An evaluation of isobaric interference corrections. *J. Anal. At. Spectrom.* **17**, 1567–1574 (2002).

51. J. D. Woodhead, J. M. Hergt, A preliminary appraisal of seven natural zircon reference materials for in situ Hf isotope determination. *Geostand. Geoanal. Res.* **29**, 183–195 (2005).
52. C. M. Fisher, J. M. Hanchar, S. D. Samson, B. Dhuime, J. Blichert-Toft, J. D. Vervoort, R. Lam, Synthetic zircon doped with hafnium and rare earth elements: A reference material for in situ hafnium isotope analysis. *Chem. Geol.* **286**, 32–47 (2011).
53. Z. Hu, Y. Liu, S. Gao, W. Liu, W. Zhang, X. Tong, L. Lin, K. Zong, M. Li, H. Chen, L. Zhou, L. Yang, Improved in situ Hf isotope ratio analysis of zircon using newly designed X skimmer cone and jet sample cone in combination with the addition of nitrogen by laser ablation multiple collector ICP-MS. *J. Anal. At. Spectrom.* **27**, 1391–1399 (2012).
54. P. H. Warren, KREEP: Major-element diversity, trace-element uniformity (almost), in *Moon in Transition: Apollo 14, KREEP, and Evolved Lunar Rocks* (Lunar and Planetary Institute, 1989), pp. 149–153.
55. C. R. Neal, G. Y. Kramer, The composition of KREEP: A detailed study of KREEP basalt 15386, paper presented at the 34th Annual Lunar and Planetary Science Conference, League City, Texas, 17 to 21 March 2003.
56. E. E. Scherer, K. L. Cameron, J. Blichert-Toft, Lu–Hf garnet geochronology: Closure temperature relative to the Sm–Nd system and the effects of trace mineral inclusions. *Geochim. Cosmochim. Acta* **64**, 3413–3432 (2000).
57. B. Efron, G. Gong, A leisurely look at the bootstrap, the jackknife, and cross-validation. *Am. Stat.* **37**, 36–48 (1983).
58. J. L. Crowley, B. Schoene, S. A. Bowring, U-Pb dating of zircon in the Bishop Tuff at the millennial scale. *Geology* **35**, 1123–1126 (2007).
59. A. H. Jaffey, K. F. Flynn, L. E. Glendenin, W. C. Bentley, A. M. Essling, Precision measurement of half-lives and specific activities of ^{235}U and ^{238}U . *Phys. Rev. C* **4**, 1889–1906 (1971).

Acknowledgments: We thank CAPTEM (Curation and Analysis Planning Team for Extraterrestrial Materials) and the Lunar Sample curators at the Johnson Space Center who made samples available for this research. We thank D. Taylor and C. Crow (University of California, Los Angeles) for originally separating and imaging the Apollo zircons; J. Hanchar for providing the synthetic zircon standards used for Hf isotopes analyses; K. Samperton for assistance measuring Lu/Hf on the Element 2 ICPMS at Princeton University; M. Grange and an anonymous reviewer for their thoughtful and helpful reviews; and K. Hodges for efficient editorial handling. **Funding:** This study was supported by National Aeronautics and Space Administration (NASA) Emerging Worlds Program grants NNX16AD35G (to K.D.M.) and NNX15AH43G (to E.D.Y.) as well as by Swiss National Science Foundation grant P300P2_147740 (to M.B.). **Author contributions:** M.B. and K.D.M. conceived the project. M.B. and P.B. developed the methods. M.B., P.B., C.B.K., I.E.K., and B.S. performed the measurements. All authors participated in the data reduction and writing of the manuscript. **Competing interests:** The authors declare that they have no competing interests. **Data and materials availability:** All data needed to evaluate the conclusions in the paper are present in the paper and/or the Supplementary Materials. Additional data related to this paper may be requested from the authors.

Submitted 26 September 2016

Accepted 29 November 2016

Published 11 January 2017

10.1126/sciadv.1602365

Citation: M. Barboni, P. Boehnke, B. Keller, I. E. Kohl, B. Schoene, E. D. Young, K. D. McKeegan, Early formation of the Moon 4.51 billion years ago. *Sci. Adv.* **3**, e1602365 (2017).